Inorg. Chem. **1987**, *26*, 862-867

Contribution from Istituto Chimico "G. Ciamician", Universitã di Bologna,
Bologna, Italy, and Istituto FRAE-CNR, Bologna, Italy

Dynamic and Static Quenching of the Luminescence of Ruthenium(II) Polypyridine Complexes by Heteropolytungstate Anions. Direct Measurements of Intramolecular Electron-Transfer Rate Constants

Roberto Ballardini,[1a] M. Teresa Gandolfi,[1b] and Vincenzo Balzani*[1]

Received July 2, 1986

The quenching of the luminescence emission intensity and lifetime of $Ru(bpy)_3^{2+}$ (bpy = 2,2'-bipyridine) and of a few other Ru(II) polypyridine complexes by the heteropolytungstate anions $Mn(OH)PW_{11}O_{39}^{6-}$ and $Co(H_2O)SiW_{11}O_{39}^{6-}$ has been studied in aqueous solution at various ionic strengths. Correlations of the quenching rate constants with the free energy change for energy or electron-transfer quenching processes indicate that the quenching takes place via an oxidative electron-transfer mechanism. Both dynamic and static quenching processes have been evidenced, and the values of the ion-pair association constants have been estimated from an elaboration of the quenching data. The rate constant for intramolecular electron transfer within the ion pairs formed by the cationic luminescent species and the anionic quencher has been experimentally obtained in some cases and estimated in others. The unusual shapes of the luminescence intensity and lifetime Stern–Volmer quenching plots obtained under certain experimental conditions are explained on the basis of ion association and ionic strength effects.

Introduction

Bimolecular outer-sphere electron-transfer reactions in fluid solution[2-5] proceed via a sequence of elementary steps, namely, formation of the precursor complex, intramolecular electron transfer within the precursor complex, and dissociation of the successor complex. The experimental kinetic measurements yield overall second-order rate constants but do not give any direct information about the act of electron transfer itself. The values of the rate constants of the intramolecular step, however, are crucial to understand the role of the various molecular parameters in determining reaction rates. Photoinduced electron-transfer processes[4-10] may offer a unique opportunity to measure or at least to evaluate the rate constants of the intramolecular step.[11] One of the strategies employed is that of studying reactions between ions of high and opposite charge to obtain substantial formation of ion pairs. Under such conditions, both dynamic and static quenching processes take place,[12-18] and this makes it also possible to evaluate association constants from simple luminescence quenching experiments.

With these aims in mind, we have studied the electron-transfer quenching of the luminescence emission of $Ru(bpy)_3^{2+}$ (bpy = 2,2'-bipyridine) and of a few other Ru(II) cationic complexes by highly charged heteropolytungstate anions (Figure 1). This paper reports a detailed description of such a study.[19]

Experimental Section

$Ru(bpy)_3Cl_2{\cdot}5H_2O$, $Ru(bpy)_2(4,4'\text{-}Cl_2bpy)(PF_6)_2$, $Ru(bpy)_2(biq)(PF_6)_2$, and $Ru(bpy)_2(DMCH)Cl_2$ (bpy = 2,2'-bipyridine; biq = 2,2'-biquinoline; DMCH = 6,7-dihydro-5,8-dimethyldibenzo[*b,j*]-1,10-phenanthroline), hereafter abbreviated as RuL_3^{2+}, were available from previous studies.[20] $K_6Co(H_2O)SiW_{11}O_{39}{\cdot}10H_2O$ and $K_6Mn(OH)PW_{11}O_{39}{\cdot}9H_2O$ (hereafter abbreviated as CoW_{11}^{6-} and MnW_{11}^{6-} or as MW_{11}^{6-}) were prepared according to published procedures.[21] Both complexes were found to lose all their hydration water molecules below 300 °C without decomposition. The electronic absorption spectra of the compounds were in agreement with those reported in the literature,[22] and the elemental analysis for Co and Mn by atomic absorption was quite satisfactory. For the cobalt compound, the elemental analysis by atomic absorption gave 6.0 ± 0.1 K atoms per molecule, while for the Mn compound the analysis gave 5.8 ± 0.1 K atoms, showing that, in agreement with previous reports,[21b] the OH ligand of the Mn compound may be partially protonated upon precipitation of the salt, in a fraction presumably depending on the pH of the mother solution.[23] At its natural pH in aqueous solution the Mn compound has apparently the same 6– charge as the cobalt compound (vide infra).

Absorption spectra were performed with a Varian Cary 219 or a Kontron Uvikon 860 spectrophotometer. Comparison between the spectra of a mixture and of its components was made by using double-room cells. Emission spectra were recorded with a Perkin-Elmer 650-40 spectrofluorometer equipped with a R928 Hamamatsu phototube. Emission lifetimes were obtained with a JK System 2000 Neodymium YAG DLPY4 laser (25-ns pulse; λ_{exc} = 355 or 532 nm) coupled with a Tektronix 7612 transient digitizer or with a modified Applied Photophysics single-photon counting apparatus (2-ns pulse; 337-nm excitation).[24] Cyclic voltammetric experiments were performed with an Amel Electrochemolab multipurpose apparatus, with a saturated calomel electrode (SCE), used as the reference electrode and a hanging mercury drop electrode (HMDF) or a stationary platinum electrode (SPE) used as the working electrode. All the experiments were carried out in aerated aqueous solutions at room temperature (~20 °C). Concentrations of the Ru complexes were in the range 5.0×10^{-6} to 5.0×10^{-5} M and that of the heteropolytungstates was between 1.0×10^{-5} and 1.0×10^{-3} M. Unless otherwise noted, the concentration of the heteropolytungstate anion was always higher than that of the Ru complex cation. Under such conditions, ion-pair associations with a RuL_3^{2+}/MW_{11}^{6-} stoichiometric ratio higher than 1 were minimized. When necessary, the ionic strength of the solution was controlled by LiCl or CsCl. The plotted τ_0/τ and I_0/I values were the average of at least three independent measurements. The values of emission intensity were corrected, in the few cases in which this was necessary, for the inner filter effect of the quencher and for geometrical factors of the spectrofluorimeter.[25] At most, the effect of this

---

(1) (a) Istituto FRAE-CNR. (b) Istituto Chimico "G. Ciamician".
(2) Marcus, R. A. *Discuss. Faraday Soc.* **1960**, *29*, 21.
(3) Sutin, N. *Prog. Inorg. Chem.* **1983**, *30*, 441.
(4) Balzani, V.; Scandola, F. In *Energy Resources by Photochemistry and Catalysis*; Graetzel, M., Ed.; Academic: London, 1983; Chapter 1, p 1.
(5) (a) Rehm, D.; Weller, A. *Ber. Bunsen-Ges. Phys. Chem.* **1969**, *73*, 834. (b) Rehm, D.; Weller, A. *Isr. J. Chem.* **1970**, *8*, 259.
(6) Balzani, V.; Bolletta, F.; Gandolfi, M. T.; Maestri, M. *Top. Curr. Chem.* **1978**, *75*, 1.
(7) Sutin, N.; Creutz, C. *Pure Appl. Chem.* **1980**, *52*, 2717.
(8) Whitten, D. G. *Acc. Chem. Res.* **1980**, *13*, 83.
(9) Endicott, J. F.; Kumar, K.; Ramasami, T.; Rotzinger, F. P. *Prog. Inorg. Chem.* **1983**, *30*, 141.
(10) Meyer, T. J. *Prog. Inorg. Chem.* **1983**, *30*, 389.
(11) Haim, A. *Comments Inorg. Chem.* **1985**, *4*, 113.
(12) Bolletta, F.; Maestri, M.; Moggi, L.; Balzani, V. *J. Phys. Chem.* **1974**, *78*, 1374.
(13) Balzani, V.; Moggi, L.; Manfrin, M. F.; Bolletta, F.; Laurence, G. S. *Coord. Chem. Rev.* **1975**, *15*, 321.
(14) Demas, J. N.; Addington, J. W. *J. Am. Chem. Soc.* **1976**, *98*, 5800.
(15) Rybak, W.; Haim, A.; Netzel, T. J.; Sutin, N. *J. Phys. Chem.* **1981**, *85*, 2856.
(16) Frank, R.; Rau, H. *J. Phys. Chem.* **1983**, *87*, 5181.
(17) White, H. S.; Becker, W. G.; Bard, A. J. *J. Phys. Chem.* **1984**, *88*, 1840.
(18) Ballardini, R.; Gandolfi, M. T.; Balzani, V. *Chem. Phys. Lett.* **1985**, *119*, 459.
(19) Preliminary results have been reported previously.[18]
(20) (a) Juris, A.; Balzani, V.; Belser, P.; von Zelewsky, A. *Helv. Chim. Acta* **1981**, *64*, 2175. (b) Juris, A.; Barigelletti, F.; Balzani, V.; Belser, P.; von Zelewsky, A. *Isr. J. Chem.* **1982**, *22*, 87.
(21) (a) Weakley, T. J. R.; Malik, S. A. *J. Inorg. Nucl. Chem.* **1967**, *29*, 2935. (b) Tourné, C. M.; Tourné, G. F.; Malik, S. A.; Weakley, T. J. R. *J. Inorg. Nucl. Chem.* **1970**, *32*, 3875.
(22) Tourné, C. M.; Tourné, G. F. *Bull. Soc. Chim. Fr.* **1969**, 1124.
(23) Zonnevijlle, F.; Tourné, C. M.; Tourné, G. F. *Inorg. Chem.* **1982**, *21*, 2742, 2751.
(24) Barigelletti, F.; Juris, A.; Balzani, V.; Belser, P.; von Zelewsky, A. *Inorg. Chem.* **1983**, *22*, 3335.

Table I. Experimental Quenching Rate Constants, Calculated Diffusion Rate Constants, and ΔG Values for the Electron- and Energy-Transfer Quenching Processes

$^*A^{2+}$	μ,[a] M	$10^{-10}k_d$,[b] $M^{-1}\ s^{-1}$	$10^{-10}k_q$,[c] $M^{-1}\ s^{-1}$		ΔG_{el}^{ox},[d] eV		ΔG_{en},[e] eV	
			MnW_{11}^{6-}	CoW_{11}^{6-}	MnW_{11}^{6-}	CoW_{11}^{6-}	MnW_{11}^{6-}	CoW_{11}^{6-}
$Ru(bpy)_3^{2+}$	1.0×10^{-4} to 1.0×10^{-3} [f]	3.8–2.9	3.8[g]	3.9[g]	−0.36	−0.22	−0.1	−1.1
	4.0×10^{-3}	2.2	2.1	2.3	−0.34	−0.20	−0.1	−1.1
	1.0×10^{-2}	1.8	1.5	1.7	−0.32	−0.18	−0.1	−1.1
	1.0×10^{-2} [h]	1.8	1.3	1.1	−0.32	−0.18	−0.1	−1.1
$Ru(bpy)_2(4,4'\text{-}Cl_2bpy)^{2+}$	1.0×10^{-4} to 1.0×10^{-3} [f]	3.8–2.9	4.5[g]	[i]	−0.23	−0.09	~0	−1.0
	4.0×10^{-3}	2.2	2.6	[i]	−0.21	−0.07	~0	−1.0
	1.0×10^{-2}	1.8	1.6	[i]	−0.19	−0.05	~0	−1.0
$Ru(bpy)_2(biq)^{2+}$	0.1	1.1	[j]	≤0.03	+0.21	+0.35	+0.3	−0.7
$Ru(bpy)_2(DMCH)^{2+}$	0.1	1.1	[j]	≤0.05	+0.11	+0.25	+0.3	−0.7

[a] Unless otherwise noted, the ionic strength was adjusted with LiCl. [b] Diffusion rate constant calculated according to the Debye–Smoluchowsky equation (Debye, P. *Trans. Electrochem. Soc.* **1942**, *80*, 5059) with use of the integration treatment reported in: Chiorboli, C.; Scandola, F.; Kisch, H. *J. Phys. Chem.* **1986**, *90*, 2211. [c] Experimental quenching rate constant obtained from the τ_0/τ Stern–Volmer plots. The uncertainty is ±10% unless otherwise noted. [d] Free energy change for the oxidative electron-transfer process (eq 6). The oxidation potentials of the excited Ru(II) complexes have been taken from ref 38; for the reduction potentials of the heteropolytungstates, see results. The ΔG values are comprehensive of the work term calculated as in ref 15. [e] Estimated from the differences between the E^{0-0} energies of the excited Ru(II) complexes[38] and the energies of the lowest excited states of CoW_{11}^{6-} and MnW_{11}^{6-}; the latter values were assumed to be equal to those of the lowest absorption levels of Co(II) and Mn(II) oxides (Jørgensen, C. K. *Adv. Chem. Phys.* **1963**, *5*, 90, 97). [f] Natural ionic strength. [g] For [Q] in the range $(1.0\text{–}5.0) \times 10^{-5}$ the τ_0/τ vs. [Q] plot was linear within the experimental uncertainty (±15%). For high quencher concentration at natural ionic strength a slight downward curvature was observed. [h] Adjusted with CsCl. [i] Nonlinear τ_0/τ plots; see text. [j] Solubility reasons prevented a significant evaluation of the rate constant.

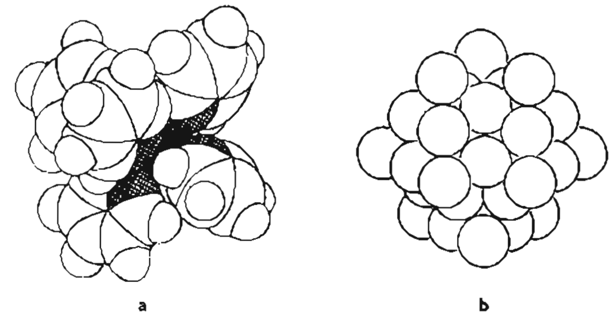

Figure 1. Schematic space-filling representations of the $Ru(bpy)_3^{2+}$ cation (a) and of the MW_{11}^{6-} heteropolytungstate anion (b).

correction was to lower the experimental value by 10%.

Results

Electrochemistry. MnW_{11}^{6-} and CoW_{11}^{6-} were found to exhibit quasi-reversible oxidation waves with $E_p = +0.88$ and $+1.00$ V vs. SCE, respectively, in agreement with previously reported values.[21b,26] These waves correspond to the one-electron oxidation of the heterometal.[21b,26] The first reduction wave, corresponding to a reversible two-electron process[26] was found to occur at $E_{1/2} = -0.88$ and -1.02 V vs. SCE for the Mn and Co complexes, respectively.

Absorption and Emission Spectra. Small but significant changes were observed in the absorption spectra of the Ru(II) complexes when their solutions were mixed with solutions containing heteropolyanions at low ionic strength ($\mu \leq 4 \times 10^{-3}$ M). The Mn compound caused slightly larger effects than the Co one. The largest effects were observed for $Ru(bpy)_2(biq)^{2+}$ and $Ru(bpy)_2(DMCH)^{2+}$, whose lower energy absorption maximum (corresponding to the Ru→biq or Ru→DMCH charge-transfer band)[20] undergoes a red shift of 6–12 nm and a decrease in ϵ_{max} of 10%. The Ru→bpy charge-transfer bands of the same complexes were much less affected. For $Ru(bpy)_3^{2+}$ and $Ru(bpy)_2(4,4'\text{-}Cl_2bpy)^{2+}$ a similar decrease in the extinction coefficient was observed, with only a small broadening of the band toward the red.

The emission spectra of $Ru(bpy)_2(biq)^{2+}$ and $Ru(bpy)_2(DMCH)^{2+}$ at very low ionic strength ($\mu \leq 1.0 \times 10^{-3}$ M) showed a red shift of 10–15 nm and an increase in the emission intensity (at constant absorption) that reached 30% when the $[RuL_3^{2+}]/[MW_{11}^{6-}]$ ratio was higher than unity. When the heteropolytungstate concentration was increased up to its solubility limit ($\leq 10^{-3}$ M), the emission intensity was found to decrease to about 80% of the initial value, while the lifetime was essentially unchanged (vide infra). For $Ru(bpy)_3^{2+}$ and $Ru(bpy)_2(4,4'\text{-}Cl_2bpy)^{2+}$, the red shift of the emission bands was less than 4 nm and there was a strong quenching effect (vide infra).

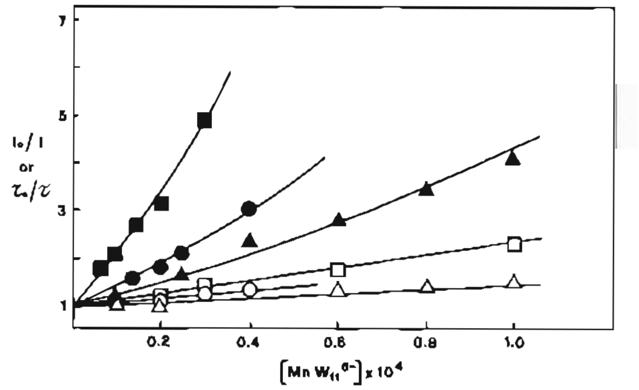

Figure 2. Stern–Volmer plots for luminescence intensity (solid symbols) and lifetime (open symbols) for the system $Ru(bpy)_3^{2+}$–MnW_{11}^{6-} at various ionic strengths ($[Ru(bpy)_3^{2+}] = 5.0 \times 10^{-6}$): (■, □) μ(natural); (●, ○) $\mu = 4.0 \times 10^{-3}$ M LiCl; (▲, △) $\mu = 1.0 \times 10^{-2}$ M LiCl.

Quenching of Emission Lifetime and Intensity. The emission lifetimes of $Ru(bpy)_2(biq)^{2+}$ (125 ns) and $Ru(bpy)_2(DMCH)^{2+}$ (140 ns) were unaffected by addition of both heteropolytungstates up to their solubility limits ($\leq 10^{-3}$ M). By contrast, the emission lifetimes of $Ru(bpy)_3^{2+}$ (400 ns) and $Ru(bpy)_2(4,4'\text{-}Cl_2bpy)^{2+}$ (175 ns) were clearly quenched. Regardless of the quencher concentration, the decay of the luminescence intensity was a single exponential when recorded with the laser equipment. In the $Ru(bpy)_3^{2+}$–CoW_{11}^{6-} system, however, under some experimental conditions the luminescence decay exhibited a two-exponential behavior when the higher resolution single-photon equipment was used.[18] When the ionic strength was kept constant, the τ_0/τ vs. [Q] Stern–Volmer plots obtained by using the single-exponential decays observed after laser excitation were linear in all the range of quencher concentration (see, e.g., Figure 2), except that for the $Ru(bpy)_2(4,4'\text{-}Cl_2bpy)^{2+}$–$CoW_{11}^{6-}$ system. For the last system, the τ_0/τ ratio generally showed a downward curvature, and at natural ionic strength, it was found to tend to a limiting value at high quencher concentrations (Figure 3). The quenching constants obtained from the linear plots under various ionic strength conditions are reported in Table I where other data, which

---

(25) Parker, C. A. *Photoluminescence of Solutions*; Elsevier: Amsterdam, 1968.

(26) Baker, L. C. W.; Figgis, J. S. *J. Am. Chem. Soc.* **1970**, *92*, 3794.

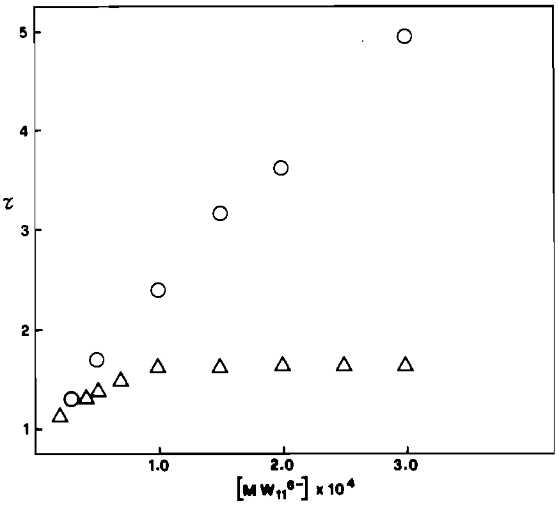

Figure 3. τ_0/τ Stern–Volmer plots for $Ru(bpy)_2(4,4'\text{-}Cl_2bpy)^{2+}$–$CoW_{11}^{6-}$ (△) and $Ru(bpy)_3^{2+}$–MnW_{11}^{6-} (○) systems at μ(natural) and $[RuL_3^{2+}] = 5.0 \times 10^{-6}$.

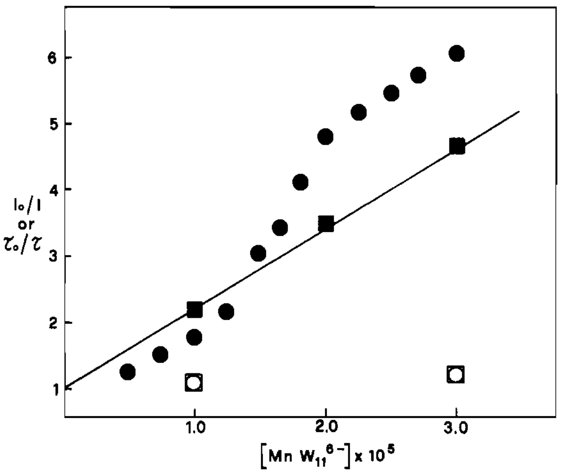

Figure 4. Stern–Volmer plots for the $Ru(bpy)_3^{2+}$–MnW_{11}^{6-} system at μ(natural) with $[Ru(bpy)_3^{2+}]/[MnW_{11}^{6-}] > 1$ and $[Ru(bpy)_3^{2+}] = 5.0 \times 10^{-5}$: (●) luminescence intensity quenching: (○) lifetime quenching. For comparison purposes, the results of experiments with $[Ru(bpy)_3^{2+}] = 5.0 \times 10^{6}$ (i.e. $[Ru(bpy)_3^{2+}]/[MnW_{11}^{6-}] < 1$) are also reported: (■) luminescence intensity quenching: (□) lifetime quenching.

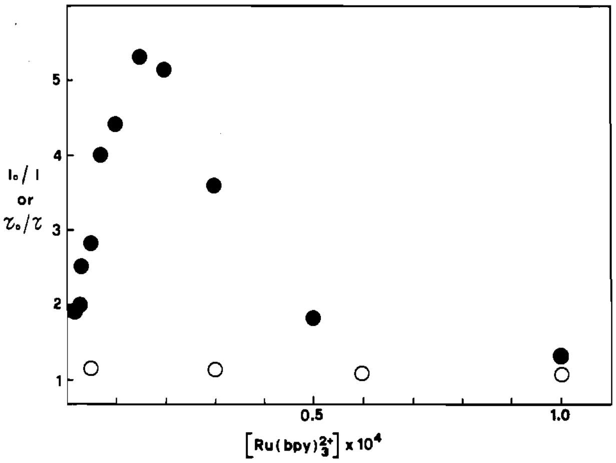

Figure 5. Changes of I_0/I and τ_0/τ for the $Ru(bpy)_3^{2+}$–$MnPW_{11}^{6-}$ system in experiments at μ(natural) and constant $[MnW_{11}^{6-}] = 1.0 \times 10^{-5}$ on changing the $Ru(bpy)_3^{2+}$ concentration: (●) emission intensity; (○) lifetime.

will be used later for the discussion, are also gathered.

The quenching of the luminescence intensity under stationary excitation in a spectrofluorimeter was also measured. As one can see from Figure 2, I_0/I vs. [Q] plots obtained in this way do not coincide with the corresponding τ_0/τ vs. [Q] plots. While most of the experiments were carried out at $[RuL_3^{2+}]/[MW_{11}^{6-}]$ ratios much smaller than unity, some experiments involving an excess of RuL_3^{2+} were also performed. Figure 4 shows the I_0/I vs. [Q] plot for $[Ru(bpy)_3^{2+}] = 5.0 \times 10^{-5}$ M and $[MnW_{11}^{6-}] \leq 3.0 \times 10^{-5}$ M. Figure 5 shows a I_0/I vs. $[Ru(bpy)_3^{2+}]$ plot at constant MnW_{11}^{6-} concentration.

Discussion

The results obtained (particularly, the strong difference between the τ_0/τ and I_0/I vs. [Q] plots, Figure 3)[12-14] clearly show that ion pairs are formed on mixing solutions of the ruthenium(II) polypyridine cations with solutions of the heteropolytungstate anions. This, of course, was expected because of the high and negative charge product and of the relatively small size of the two ions. An estimation of the association constant K can be obtained from eq 1–3,[15,27] where a is the distance between the centers of

$$K = \frac{4\pi N a^3}{3000} \exp(-w/RT) \qquad (1)$$

$$w = \frac{z_A z_B e^2 N}{Da(1 + \beta a \mu^{1/2})} = \frac{w_0}{(1 + \beta a \mu^{1/2})} \qquad (2)$$

$$\beta = \left(\frac{8\pi N e^2}{1000DkT}\right)^{1/2} \qquad (3)$$

the two species, z_A and z_B are the ionic charges, D is the static dielectric constant of water, k is the Boltzmann constant, and μ is the ionic strength. Taking a equal to the sum of the radii r_A and r_B of the complexes (~0.70 nm for $Ru(bpy)_3^{2+}$ [28] and ~0.55 nm for the heteropolytungstate anions[29]), the resulting values of K are 3500, 2100, 1120, and 630 M^{-1} at ionic strengths 1.0×10^{-4}, 1.0×10^{-3}, 4.0×10^{-3}, and 1.0×10^{-2} M, respectively. As we will see later, the results obtained in our experiments indicate that the values of the association constants are, in fact, much larger.

Effects of Ion-Pair Formation on Absorption and Emission Spectra. Ion-pair formation causes small but significant effects on the spectroscopic properties of the ruthenium(II) polypyridine complexes. This was expected because other authors[16,30-33] had previously reported that the absorption and emission spectra of $Ru(bpy)_3^{2+}$ can be used to monitor the nature of its environment. The red shifts of the metal-to-ligand charge-transfer absorption bands and of the corresponding luminescence emission indicates that the π (t_{2g} in octahedral symmetry) Ru orbitals move to higher energy upon ion-pairing. Although such an effect can indirectly derive from an interaction between the heteropolytungstate anion and the ligands of the Ru complexes, a direct interaction of the anion with the central metal of the cationic complexes cannot be excluded. Inspection of molecular models shows that the polytungstate anion can substantially penetrate the "pockets" of the Ru–polypyridine structure[34] (Figure 1), so that a peripherical oxygen of the anionic complex can arrive at a very small distance from the central metal of the cationic complex. As we will see later, such a penetration is consistent with the values obtained for the association constants. The fact that in the mixed ligand $Ru(bpy)_2(biq)^{2+}$ and $Ru(bpy)_2(DMCH)^{2+}$ complexes the Ru→biq and Ru→DMCH bands are more affected than the Ru→bpy

---

(27) Fuoss, R. M. *J. Am. Chem. Soc.* **1958**, *80*, 5059.

(28) Sandrini, D.; Gandolfi, M. T.; Maestri, M.; Bolletta, F.; Balzani, V. *Inorg. Chem.* **1984**, *23*, 3017.

(29) Pope, M. T. *Heteropoly and Isopoly Oxometalates*; Springer Verlag: West Berlin, 1983.

(30) Meisel, D.; Matheson, M. S.; Rabani, J. *J. Am. Chem. Soc.* **1978**, *100*, 117.

(31) Wheeler, J.; Thomas, J. K. *J. Phys. Chem.* **1982**, *86*, 4540.

(32) Chu, D. Y.; Thomas, J. K. *J. Phys. Chem.* **1985**, *89*, 4065.

(33) Yersin, H.; Hensler, G.; Gallhuber, E.; Rettig, W.; Schwan, L. O. *Inorg. Chim. Acta* **1985**, *105*, 201.

(34) Rillema, D. P.; Jones, D. S.; Levy, H. A. *J. Chem. Soc., Chem. Commun.* **1979**, 849.

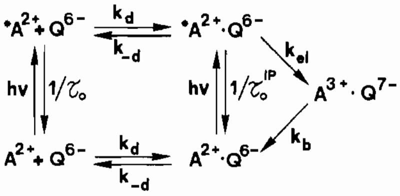

Figure 6. Kinetic scheme for the oxidative electron-transfer quenching process.

bands suggests that the anion prefers to approach the cation on the side of the smaller bpy ligands.

For the $Ru(bpy)_2(biq)^{2+}$ and $Ru(bpy)_2(DMCH)^{2+}$ excited states, the emission lifetime is substantially unaffected by ion pairing, whereas the emission intensity increases slightly for $[RuL_3^{2+}]/[MW_{11}^{6-}]$ ratios higher than unity and decreases slightly for reversed concentration ratios. Emission intensity and lifetime are given by $I_0 \propto \eta k_{em}/(k_{em} + k_{nr})$ and $\tau_0 = 1/(k_{em} + k_{nr})$, where η is the efficiency of population of the emitting excited state and k_{em} and k_{nr} (with $k_{nr} >> k_{em}$)[35] are the radiative and nonradiative deactivation rate constants. Since in these cases the lifetime is not affected by ion pairing, k_{nr} is practically constant and the changes in the emission intensity must be due to changes in either η or k_{em} upon ion pairing. Since η is expected to be unity in the unpaired Ru(II) complexes[36-38] it seems more likely that ion pairing affects the radiative rate constant k_{em}, as is also indicated by the changes observed in the absorption spectra.

Quenching Mechanism. It is well-known[6-9,13] that efficient quenching of electronically excited states may take place by either energy or electron transfer. In our systems these quenching processes may be written as follows:

energy transfer

$$*RuL_3^{2+} + MW_{11}^{6-} \rightarrow RuL_3^{2+} + *MW_{11}^{6-} \qquad (4)$$

reductive electron transfer

$$*RuL_3^{2+} + MW_{11}^{6-} \rightarrow RuL_3^{+} + MW_{11}^{5-} \qquad (5)$$

oxidative electron transfer

$$*RuL_3^{2+} + MW_{11}^{6-} \rightarrow RuL_3^{3+} + MW_{11}^{7-} \qquad (6)$$

Both the Co(II) and Mn(II) centers possess low-energy excited states so that the energy-transfer process is energetically allowed in all cases except for $Ru(bpy)_2(biq)^{2+}$ and $Ru(bpy)_2(DMCH)^{2+}$ with MnW_{11}^{6-} (Table I). Reductive electron transfer is always thermodynamically forbidden,[39] while oxidative electron transfer is thermodynamically allowed for $Ru(bpy)_3^{2+}$ and $Ru(bpy)_2(4,4'\text{-}Cl_2\,bpy)^{2+}$. The values of the quenching constants suggest that only oxidative electron transfer is effective. The lack of energy-transfer quenching under thermodynamically favorable conditions, (see, for example, the $Ru(bpy)_2(biq)^{2+}$–CoW_{11}^{6-} system) indicates that this process is slow for kinetic reasons. This is in agreement with the generally observed nonadiabatic behavior of energy-transfer processes involving metal-centered excited states.[40,41] Furthermore, in the present systems the overlap between the metal and ligand orbitals of the Ru complex and the Co(II) or Mn(II) orbitals of the polytungstate anion is disfavored by statistical reasons (the heterometal occupies one of the 12 peripherical octahedric sites of the heteropolytungstate anion) and, presumably, is also disfavored because the presence of hydrogen atom(s) on the external oxygen atom bound to the hetero metal makes this site less available to the ion-pair interaction.

Dynamic and Static Quenching. Electron-transfer quenching of excited states in a system involving ion-pair formation can be discussed on the basis of the scheme shown in Figure 6,[15,16,18] which differs from the simpler scheme proposed by Rehm and Weller for dynamic quenching[5] because it takes into account the light absorption and emission by the ion pairs. In the scheme of Figure 6, k_d and k_{-d} are the diffusion-controlled rate constants for the formation and dissociation of the precursor complex, K is the ion-pair formation constant (assumed to be equal to k_d/k_{-d}), k_{el} and k_b are the rate constants for electron transfer in the precursor and successor complex, and τ_0 and τ_0^{IP} are the lifetimes due to radiative and nonradiative (excepting electron transfer) deactivation of the "free" and "paired" excited state. Since the lifetimes of $*Ru(bpy)_2(biq)^{2+}$ and $*Ru(bpy)_2(DMCH)^{2+}$, which are not quenched by the heteropolytungstate anions, are not affected by ion-pairing, we can safely assume in the following that τ_0^{IP} is the same as τ_0. On the basis of our results, we can also assume that the extinction coefficients of the "free" and "paired" Ru(II) complexes are approximately equal. Finally, an implicit assumption of the scheme is that the precursor complex of the dynamic quenching coincides with the excited preformed ion pair. It has been recently pointed out that this last assumption may be not correct for nonspherical systems, e.g. when at least one of the two partners is a species showing an anisotropic distribution of electric charges and redox reactive centers.[42]

For the simple case of quenching without ion-pair formation, the well-known relationships[13]

$$I_0/I = 1 + k_q\tau_0[Q] \qquad (7)$$

$$\tau_0/\tau = 1 + k_q\tau_0[Q] \qquad (8)$$

are obeyed and the intensity and lifetime Stern–Volmer plots coincide. When ion pairs are formed, the scheme of Figure 6 yields the following complicated relationship for I_0/I vs. [Q]:[15,16]

$$\frac{I_0}{I} = \frac{(1 + k_q\tau_0[Q])(1 + K[Q])}{1 + C[Q]} \qquad (9)$$

where

$$C = \frac{k_{-d}K + (k_{em}^{IP}/k_{em})\{(1/\tau_0 + k_d[Q])K + k_d\}}{1/\tau_0^{IP} + k_{el} + k_{-d}}$$

In eq 9, k_{em}^{IP} and k_{em} are the rate constants for emission by the ion pair and by the free Ru complex, respectively, and k_q is given by

$$k_q = \left(\frac{k_d k_{el}}{k_{el} + k_{-d}}\right)\frac{1 + 1/(\tau_0^{IP}k_{el})}{1 + 1/\{\tau_0^{IP}(k_{el} + k_{-d})\}} \qquad (10)$$

Equation 9 obviously reduces to eq 7 when ion pairs are not present. When $k_{el} >> 1/\tau_0^{IP} + k_{-d}$, the dynamic quenching process is diffusion-controlled ($k_q = k_d$) and the ion pairs do not emit. Under such conditions, $C[Q]$ may be much smaller than unity even for sufficiently high Q concentrations. In such a case eq 9 reduces to

$$I_0/I = (1 + k_q\tau_0[Q])(1 + K[Q]) \qquad (11)$$

This equation was previously used[12-14] in conjunction with eq 8 to estimate the values of ion-pair association constants from luminescence quenching experiments.

The more exergonic is the quenching process, the more the approximations that lead to eq 11 are expected to hold true since k_{el} increases with increasing exergonicity. For the Ru-

---

(35) At room temperature the quantum yield of luminescence emission is much lower than unity because of fast thermally activated radiationless deactivation processes.[24,36-38]

(36) Kalyanasundaram, K. *Coord. Chem. Rev.* **1982**, *46*, 159.

(37) Watts, J. R. *J. Chem. Educ.* **1983**, *60*, 834.

(38) Balzani, V.; Juris, A.; Barigelletti, F.; Belser, P.; von Zelewsky, A. *Riken Q.* **1984**, *78*, 78.

(39) In the most favorable case (electron transfer from MnW_{11}^{6-} to $Ru(bpy)_2(4,4'\text{-}Cl_2bpy)^{2+}$ at $\mu = 1.0 \times 10^{-4}$ M) ΔG for reductive intramolecular electron transfer (eq 5) is +0.09 eV. For the reduction potentials of excited Ru(II) complexes see ref 38; for the oxidation potentials of the heteropolytungstates, see Results.

(40) Scandola, F.; Balzani, V. *J. Chem. Educ.* **1983**, *60*, 814.

(41) Gandolfi, M. T.; Maestri, M.; Sandrini, D.; Balzani, V. *Inorg. Chem.* **1983**, *22*, 3435.

(42) Balzani, V.; Juris, A.; Scandola, F. In *Homogeneous and Heterogeneous Photocatalysis*; Pelizzetti, E., Serpone, N., Eds.; D. Reidel: Dordrecht, 1986; p 1.

Table II. Association Constants and Intramolecular Electron-Transfer Rate Constants

		K_{exptl},[b] M^{-1}			k_{el},[d] s^{-1}	
$*A^{2+}$	μ,[a] M	MnW_{11}^{6-}	CoW_{11}^{6-}	K_{calcd},[c] M^{-1}	MnW_{11}^{6-}	CoW_{11}^{6-}
$Ru(bpy)_3^{2+}$	1.0×10^{-4} to 1.0×10^{-3} [e]	$(7.4 \pm 1.0) \times 10^4$	$(5.4 \pm 1.0) \times 10^4$	6.2×10^4		
	4.0×10^{-3} [e]	3.7×10^4	3.0×10^4	2.2×10^4	$\geqslant 5.0 \times 10^8$ [f]	8.5×10^7 [g]
	4.0×10^{-3}	3.1×10^4	1.6×10^4	2.2×10^4		
	1.0×10^{-2}	1.7×10^4	8.6×10^3	1.1×10^4		
	1.0×10^{-2} [h]	9.2×10^3	4.4×10^3	1.1×10^4		
$Ru(bpy)_2(4,4'\text{-}Cl_2bpy)^{2+}$	1.0×10^{-4} to 1.0×10^{-3} [e]	$(7.5 \pm 1.0) \times 10^4$	*i*	6.2×10^4		
	4.0×10^{-3}	2.7×10^4	*i*	2.2×10^4	$\geqslant 1.0 \times 10^8$ [f]	$\sim 4 \times 10^6$ [j]
	1.0×10^{-2}	1.7×10^4	*i*	1.1×10^4		

[a] The ionic strength was adjusted with LiCl, unless otherwise noted. [b] Experimental association constants derived from the luminescence quenching experiments (see Discussion). The uncertainty was ±20%, unless otherwise indicated. [c] Association constants calculated from the k_d/k_{-d} ratio by using the Fuoss equation[27] with $a = 0.75$ nm. [d] Rate constant for electron transfer in the ion pair. [e] Natural ionic strength. [f] Estimated from the best fitting procedure on I_0/I plots; these limiting values hold true also in the other experimental conditions used; see Discussion. [g] Experimentally measured from the double-exponential lifetime decay, see Discussion. [h] Adjusted with CsCl. [i] Nonlinear τ_0/τ plots; see text. [j] Obtained from the τ_0/τ plateau value; see Discussion.

$(bpy)_3^{2+}$–MnW_{11}^{6-} and $Ru(bpy)_2(4,4'\text{-}Cl_2bpy)^{2+}$–$MnW_{11}^{6-}$ systems at low ionic strength ($\mu \leqslant 0.01$ M) (i) a single exponential decay has been obtained, (ii) the quenching constants obtained from eq 8 are in agreement with those calculated for diffusion controlled processes (Table I), and (iii) the experimental I_0/I vs. [Q] plots can be fitted by eq 11. For these systems the values of the association constant K were obtained by a best fitting of eq 11 to the experimental I_0/I, k_q, and τ_0 values. These values (see Table II) are much higher than those calculated by eq 1–3 when the sum of the radii of the two complexes is used as the distance between the centers of the two species (vide supra). This disagreement is quite understandable because the heteropolytungstate anion can deeply penetrate into the pockets of the Ru–polypyridine structure.[34] With molecular models (Figure 1), it can be seen that this penetration can reduce the center-to-center distance from 1.25 nm (which is the sum of the radii of the two complexes) to about 0.8–0.9 nm. To obtain K_{calcd} values of the same size of the K_{exptl} values (Table II), one should use a value of 0.75 nm for a in eq 1–3 (note, however, that such equations are only valid for spherical reactants in contact).

The same behavior was observed for the $Ru(bpy)_3^{2+}$–CoW_{11}^{6-} system at low ionic strength (μ(natural) = 1.0×10^{-4} to 1.0×10^{-3} M), that is (i) the emission decayed according to a single exponential, (ii) $k_q = k_d$, and (iii) eq 11 fitted well the experimental I_0/I vs. [Q] plot. The value obtained for the association constant was somewhat smaller than that found for the $Ru(bpy)_3^{2+}$–MnW_{11}^{6-} system. This result is consistent with the fact that the radius of $Co(H_2O)SiW_{11}O_{39}^{6-}$ is expected to be slightly higher than that of $Mn(OH)PW_{11}O_{39}^{6-}$ because the tetrahedral Si–O bonds are slightly longer than the analogous P–O bonds.[29,43] For higher natural ionic strength, the K_{exptl} values obtained for this system (not shown in Table II) differed more and more from those of the analogous $Ru(bpy)_3^{2+}$–MnW_{11}^{6-} and $Ru(bpy)_2(4,4'\text{-}Cl_2bpy)^{2+}$–$MnW_{11}^{6-}$ systems as the ionic strength increased. Furthermore, an accurate analysis of the luminescence decay showed, at least under some conditions, a double-exponential decay. These facts were taken as signals that the approximations introduced (C[Q] << 1) to reduce eq 9 to eq 11 were no longer tolerable. This could be expected because (a) for CoW_{11}^{6-} the electron-transfer reaction is less exergonic (and thus slower) than that for MnW_{11}^{6-}, (b) for high ionic strength k_{-d} increases, and (c) at higher ionic strength higher quencher concentrations had to be used. As reported previously,[18] for [Q] = 2.0×10^{-4} and μ(natural) = 4.0×10^{-3} M the double-exponential decay yielded experimental decay constants $-m_1 = 8.9 \times 10^7$ s^{-1} and $-m_2 = 9.6 \times 10^6$ s^{-1}, which have to be close to k_{el} and k_d[Q], respectively.[44] With $k_{\text{el}} = 8.5 \times 10^7$ s^{-1} the value of C[Q] in the denominator of eq 9 is not negligible for the experiments with μ(natural) > 1.0×10^{-3} M.[45] In these cases we have introduced the experimental k_q, τ_0, and k_{el} values into the complete eq 9 to obtain the K_{exptl} values given in Table II. Incidentally, it can be noticed that LiCl exhibits a somewhat different effect on the K_{exptl} of $Ru(bpy)_3^{2+}$–MnW_{11}^{6-} and $Ru(bpy)_3^{2+}$–CoW_{11}^{6-} systems. An interesting point is that the data concerning the $Ru(bpy)_3^{2+}$–MnW_{11}^{6-} and $Ru(bpy)_2(4,4'\text{-}Cl_2bpy)^{2+}$–$MnPW_{11}^{6-}$ systems are best fitted by k_{el} values higher than that found for the $Ru(bpy)_3^{2+}$–CoW_{11}^{6-} system, i.e. $k_{\text{el}} \geqslant 1.0 \times 10^8$ s^{-1} for the $Ru(bpy)_2(4,4'\text{-}Cl_2bpy)^{2+}$–$MnW_{11}^{6-}$ system and $k_{\text{el}} \geqslant 5.0 \times 10^8$ s^{-1} for the $Ru(bpy)_3^{2+}$–MnW_{11}^{6-} system. This is in agreement with the larger exergonicity of the electron-transfer reactions involving MnW_{11}^{6-} and also with the lact of a two-exponential decay in these systems because the rate of the ion-pair decay must be faster than the time resolution of our experimental setup.

Finally, for the $Ru(bpy)_2(4,4'\text{-}Cl_2bpy)^{2+}$–$CoW_{11}^{6-}$ system, the rate of decay of excited ion pairs is expected to be the slowest one because of thermodynamic reasons (Table I). For this system, the luminescence was found to decay according to a single exponential. However, the τ_0/τ vs. [Q] plots exhibited a downward curvature. When the ionic strength was controlled, the quencher concentration had to be limited and the maximum quenching effect observed was 30%. At uncontrolled ionic strength, the τ_0/τ vs. [Q] plot was found to reach a plateau value at $\tau_0/\tau = 1.7$ (Figure 3). As one can see from the other plot of the same figure, the ionic strength effect on the diffusion rate constant is almost negligible in this concentration range, showing that the plateau originates from a saturation effect intrinsic to the $Ru(bpy)_2(4,4'\text{-}Cl_2bpy)^{2+}$–$CoW_{11}^{6-}$ system. We believe that in this system the quenching limiting factor at high Q concentration becomes the rate of the intramolecular electron transfer step (k_{el}). From the values of the association constant of the other analogous systems one can see that at the [Q] values for which the plateau is reached (i) at least 80% of the $Ru(bpy)_2(4,4'\text{-}Cl_2bpy)^{2+}$ ions have to be paired with CoW_{11}^{6-} and (ii) k_{-d} has to be smaller than $1/\tau_0^{\text{IP}}$. Thus, the observed τ(plateau) is substantially the lifetime of the excited ion pair, and the value of k_{el} can be estimated from

$$1/\tau(\text{plateau}) \simeq 1/\tau_0^{\text{IP}} + k_{\text{el}} \qquad (12)$$

With $1/\tau(\text{plateau}) \simeq 1 \times 10^7$ s^{-1} and $1/\tau_0^{\text{IP}} = 5.8 \times 10^6$ s^{-1}, the result is $k_{\text{el}} \simeq 4 \times 10^6$ s^{-1}.

Ionic Strength and Concentration Effects. As expected when charged species are involved, we have observed ionic strength and concentration effects in our quenching experiments.

An increase in the ionic strength was found to decrease the quenching constants (Figure 2 and Table I) as well as the ion-pair association constants (Table II). Furthermore, specific ion effects were observed. In the quenching of $*Ru(bpy)_3^{2+}$ by MnW_{11}^{6-}

---

(43) For center-to-center distances $a < 0.9$ nm the value of the association constant is extremely sensitive to small changes in the value of a.

(44) Two distinct exponential decays were also observed for [Q] = 4.0×10^{-4} and μ(natural) = 8.0×10^{-3} M; m_1 was essentially the same at the two different Q concentrations as expected for an intramolecular decay. For the kinetic scheme and for other details see ref 18.

(45) Although the values of the intramolecular electron-transfer rate constant could depend on the ionic strength,[15,46] to a first approximation we assume that the $k_{\text{el}} = 8.5 \times 10^7$ s^{-1} value found for $\mu = (4–8) \times 10^{-3}$ M can be used in the whole ionic strength range used ($\mu \leqslant 1.0 \times 10^{-2}$ M).

(46) Kondo, S.; Sasaki, Y.; Saito, K. *Inorg. Chem.* **1981**, *20*, 429.

or CoW_{11}^{6-}, when 0.01 M LiCl was replaced by 0.01 M CsCl as the ionic-strength-controlling electrolyte, K_{exptl} was reduced to one-half (Table II) and k_q ($=k_d$) was reduced by about 30% (Table I).

While most of the experiments were carried out at $[RuL_3^{2+}]/[MW_{11}^{6-}]$ ratios much smaller than unity (vide supra), in some experiments an excess of RuL_3^{2+} was used. Figure 4 shows that under such conditions the I_0/I vs. [Q] Stern–Volmer plot for the $Ru(bpy)_3^{2+}$–MnW_{11}^{6-} system exhibits a quite peculiar shape, in contrast with the linear shape of the plot obtained when the MnW_{11}^{6-} quencher is in excess with respect to the $Ru(bpy)_3^{2+}$. In contrast, the τ_0/τ vs. [Q] plot is the same, regardless of the excess species. This shows that the different behavior of the I_0/I vs. [Q] plots has to be due to static quenching effects. The very peculiar behavior of the I_0/I vs. [Q] plot for $[Ru(bpy)_3^{2+}]/[MnPW_{11}^{6-}]$ ratios higher than unity is likely to be caused by the presence of variable amounts of 1:1 and 2:1 associated species. In the latter species, the same MnW_{11}^{6-} ion can quench statically two different $Ru(bpy)_3^{2+}$ excited states. The presence of such RuL_3^{2+}–MW_{11}^{6-}–RuL_3^{2+} ion triplets has been confirmed by high-intensity laser excitation experiments where the annihilation reaction of two RuL_3^{2+} excited states has been observed.[47]

The peculiar shape of the I_0/I vs. $[Ru(bpy)_3^{2+}]$ plot at constant (1.0×10^{-5} M) MnW_{11}^{6-} concentration (Figure 5) is also worth noticing. For an ideal system where only dynamic quenching takes place and the ionic strength is constant, I_0/I would be constant at any $Ru(bpy)_3^{2+}$ concentration and coincident with the τ_0/τ plot. Under the experimental conditions used (Figure 5) the ionic strength changed slightly (as shown by the slight changes in the τ_0/τ ratio). The observed large changes in the I_0/I ratio with increasing $[Ru(bpy)_3^{2+}]$ must thus be due again to static quenching effects. Clearly, there is an increase of the contribution of the static quenching with increasing $Ru(bpy)_3^{2+}$ concentration for $[Ru(bpy)_3^{2+}]/[MnW_{11}^{6-}]$ ratios lower than unity and then a decrease at higher $[Ru(bpy)_3^{2+}]$ concentrations. This behavior should reflect the different fractions of free $Ru(bpy)_3^{2+}$ and of 1:1 and 2:1 associated species. For $[Ru(bpy)_3^{2+}] \rightarrow \infty$, the I_0/I value should reflect the quenching of associated species with high $[Ru(bpy)_3^{2+}]/[MnW_{11}^{6-}]$ stoichiometric ratios on free $Ru(bpy)_3^{2+}$ excited states (i.e., it practically should tend to unity). For $[Ru(bpy)_3^{2+}] \rightarrow 0$, I_0/I should reach the value imposed by the static quenching in the 1:1 ion pair.

Conclusions

By an appropriate choice of polypyridine–Ru(II) complex cations and heteropolytungstate anions we have been able to obtain systems in which the rate of electron-transfer quenching of the excited Ru complex can be tuned. Values of the ion-pair association constants have been obtained under various experimental conditions, and the effects of reactant concentration and ionic strength on the dynamic and static quenching processes have been investigated.

Taking advantage of the extensive formation of ion pairs, rate constants of intramolecular electron-transfer quenching processes have been directly measured or evaluated.

Acknowledgment. We thank Prof. A. von Zelewsky and Dr. P. Belser for samples of some of the Ru(II) complexes, Dr. M. Ciano for the electrochemical measurements, Prof. M. Maestri for the computer programs, and Dr. M. Taddia for atomic absorption analyses. We also thank G. Gubellini for technical assistance. Partial support from Ministero della Pubblica Istruzione is gratefully acknowledged.

Registry No. $Ru(bpy)_3Cl_2$, 14323-06-9; $Ru(bpy)_2(4,4'\text{-}Cl_2bpy)(PF_6)_2$, 75778-18-6; $Ru(bpy)_2(biq)(PF_6)_2$, 75777-91-2; $Ru(bpy)_2(DMCH)Cl_2$, 105817-79-6; $K_6Co(H_2O)SiW_{11}O_{39}$, 105785-76-0; $K_6Mn(OH)PW_{11}O_{39}$, 105834-58-0.

Supplementary Material Available: Tables reporting lifetime and intensity quenching data (3 pages). Ordering information is given on any current masthead page.

---

[47] In such experiments, which will be reported elsewhere, RuL_3^{2+} was $Ru(bpy)_2(biq)^{2+}$ or $Ru(bpy)_2(DMCH)^{2+}$.

Contribution from the Chemistry Center, IVIC, Caracas 1020-A, Venezuela,
Chemistry Department, Universidad Simõn Bolivar, Caracas 1080-A, Venezuela,
and Istituto Chimico "G. Ciamician", University of Bologna, Bologna 40126, Italy

Interaction of $(\mu\text{-}H)_4Ru_4(CO)_{12}$ with Diphosphines in the Presence of Trimethylamine *N*-Oxide. X-ray Crystal Structure Analyses of $(\mu\text{-}H)_4Ru_4(CO)_{10}(\mu\text{-}\{Ph_2P(CH_2)_nPPh_2\})$ (n = 1, 3, 4), $(\mu\text{-}H)_4Ru_4(CO)_{10}(\mu\text{-}\{Ph_2PCH_2CH(CH_3)PPh_2\})$, and $(\mu\text{-}H)_4Ru_4(CO)_{10}(\{Ph_2PCH_2CH(CH_3)PPh_2\})$

Josẽ Puga,*[1a] Alejandro Arce,[1b] Dario Braga,*[1c] Nicola Centritto,[1b] Fabrizia Grepioni,[1c]
Rafael Castillo,[1a] and Julian Ascanio[1a]

Received June 2, 1986

The complexes $(\mu\text{-}H)_4Ru_4(CO)_{10}(\mu\text{-}\{Ph_2P(CH_2)_nPPh_2\})$ (n = 1 (**1**), 3 (**3**), 4 (**4**)), $(\mu\text{-}H)_4Ru_4(CO)_{10}(\mu\text{-}\{Ph_2PCH_2CH(CH_3)PPh_2\})$ (**2a**), $(\mu\text{-}H)_4Ru_4(CO)_{10}\{Ph_2PCH_2CH(CH_3)PPh_2\}$ (**2b**), and $[(\mu\text{-}H)_4Ru_4(CO)_{11}]_2\{Ph_2P(CH_2)_5PPh_2\}$ (**5a**) have been characterized by IR, ^1H NMR, and ^{31}P NMR spectroscopy. The structures of compounds **1**, **2a**, **2b**, **3**, and **4** have been determined by single-crystal X-ray diffractometry. The diphosphine ligands are seen to bridge a Ru–Ru bond of the tetrahedral Ru_4 cluster in **1**, **2a**, **3**, and **4**, while the diphosphine ligand adopts a chelating mode of bonding in **2b**. The hydride atoms in each of the structures were not located but were inferred from Ru–Ru bond lengths. They take up the same distribution of idealized C_s symmetry in all four structures. Where an asymmetric carbon atom is present (**2a** and **2b**) only one of the two possible diastereoisomeric forms is found in the solid. Crystal data: for **1**, a = 10.967 (5) Å, b = 19.720 (3) Å, c = 18.430 (3) Å, β = 104.56 (3)°, space group $P2_1/c$, Z = 4, final R = 0.055, R_w = 0.056; for **2a**, a = 17.79 (1) Å, b = 20.419 (6) Å, c = 11.395 (4) Å, β = 106.84 (5)°, space group Cc, Z = 4, final R = 0.038, R_w = 0.039; for **2b**, a = 11.219 (5) Å, b = 13.229 (2) Å, c = 15.226 (3) Å, α = 92.59 (2)°, β = 93.21 (2)°, γ = 100.99 (2)°, space group $P\bar{1}$, Z = 2, final R = 0.054, R_w = 0.059; for **3**, a = 8.783 (1) Å, b = 21.133 (6) Å, c = 22.140 (2) Å, β = 90.96 (1)°, space group $P2_1/c$, Z = 4, final R = 0.048, R_w = 0.049; for **4**, a = 8.918 (1) Å, b = 21.701 (3) Å, c = 22.131 (4) Å, β = 100.47 (1)°, space group Cc, Z = 4, final R = 0.034, R_w = 0.035.

Introduction

Tetranuclear carbonyl cluster have been shown to be useful catalysts, or catalyst precursors, for hydrogenation reactions.[2,3] Incorporation of bidentate phosphines within the metal framework configuration could be used, in some instances to maintain the

---

[1] (a) IVIC. (b) Universidad Simõn Bolivar. (c) University of Bologna.

[2] Sãnchez-Delgado, R. A.; Puga, J.; Rosales, M. *J. Mol. Catal.* **1984**, *24*, 221

0020-1669/87/1326-0867$01.50/0